A Transpiration-Cooled Nozzle as Applied to a Gas-Core Nuclear Propulsion System

E. L. KRAMER* AND S. GRONICH†
Douglas Aircraft Co., Inc., Santa Monica, Calif.

The use of mass injection through a porous wall as a cooling technique for axisymmetric nozzles is investigated. The effect of homogeneous mass injection on the heat transfer in a turbulent, compressible boundary layer is analyzed, using an integral-momentum approach. Approximate formulations of the gaseous thermal radiative and recombination energy contributions are included in the analysis. Coolant requirements are determined for a conical nozzle associated with a 10^6 lb-thrust gas-core system operating at a 300-atm chamber pressure. Hydrogen is assumed to be used for the propellant and coolant. Chamber temperatures range from 7500° to 20,000°R, and wall temperatures range from 2000° to 3000°R. The degradation of specific impulse, which is a result of expelling the coolant at a lower total temperature than that in the chamber, is found to be as high as 9% at 20,000°R for a wall temperature of 2000°R.

Nomenclature

a = wall thickness, ft
B = Btu
c = velocity of light, fps
C_f = skin friction
C_p = specific heat at constant pressure, B/lbm-°R
d = pore diameter, ft
$E_{B\omega}$ = Planck's function, erg/sec-cm
F = blowing parameter, $F = G/\rho_\infty U_\infty$; thrust, lbf
g = gravitational constant
G = coolant mass velocity, lbm/ft²-sec
H = propellant enthalpy, B/lbm
h = heat transfer coefficient, B/ft²-sec-°R; Planck's constant
I_{sp} = specific impulse, sec
k = permeability coefficient, ft²
K = thermal conductivity, B/ft-sec-°R; Boltzmann's constant
Le = Lewis number
M = freestream Mach number
m = molecular weight, lbm/lb-mole
N_t = total number of coolant tubes
n = velocity exponent
P = porosity
$P_{(\text{subscript})}$ = pressure, lbf/ft²
Pr = Prandtl number
$\dot{q}$ = heat flux, B/ft²-sec
r_0 = recovery factor
R = gas constant, ft-lbf/lbm-°R
St = Stanton number (with cooling)
St_0 = Stanton number (without cooling)
t = coolant temperature, °R
T = propellant temperature, °R
U = gas velocity in x direction, fps
V = gas velocity in y direction, fps
$\dot{w}$ = flow rate, lbm/sec
x = distance measured along nozzle surface, ft; mole fraction
y = distance measured normal to wall, ft
z = axial distance, ft
α = viscous resistance, ft^{-2}
α_ν = monochromatic absorptivity of wall
$\bar{\alpha}_W$ = average wall absorptivity
δ = boundary-layer thickness, ft
δ^* = displacement thickness, ft
$\bar{\epsilon}_W$ = average wall emissivity
ϵ = area ratio
κ = absorption coefficient, ft^{-1}
μ = viscosity, lbm/ft-sec
ρ = density, lbm/ft³
θ = momentum thickness, ft
ω = viscosity exponent; wave number, cm^{-1}
γ = specific heat ratio

Subscripts

AW = adiabatic wall
c = coolant
C = convective
CH = chamber
ci = coolant inlet
0 = propellant
R = radiative
th = throat
$W0$ = wall (coolant side)
W = wall (gas side)
∞ = freestream
1 = atomic species
2 = molecular species
* = reference temperature

Introduction

THE current impetus towards high-temperature, high-performance propulsion systems has introduced unique problems associated with the design of rocket-nozzle cooling systems. Typical of these problems is that of designing for the high heat fluxes produced in the nozzle by hydrogen when used in conjunction with a nuclear reactor power source. Previous studies[1, 2] have indicated that pure regenerative convective cooling by H_2 can be applied successfully to the nozzle of a solid-core reactor system (chamber temperatures up to about 5000°R). As will be seen, regenerative cooling is applicable only up to chamber temperatures of the solid-core system.

An attempt to circumvent the material limitations of the solid-core system in order to achieve higher specific impulses resulted in the concept of the gaseous-core reactor, in which the fissionable material is maintained in the gaseous state, and energy is transferred to the propellant primarily by thermal radiation. Preliminary analyses have indicated that chamber temperatures and pressures of the order of 10,000°R and 300 atm will be required, based on heat transfer and nuclear considerations.[3] The effect on the maximum heat flux in the

Presented as Preprint 64-544 at the AIAA Aerospace Propulsion Meeting, Cleveland, Ohio, May 4–6, 1964; revision received January 8, 1965.
* Research Engineer, Nuclear Department, Missile and Space Systems Division.
† Chief Scientist, Nuclear Department, Missile and Space Systems Division. Member AIAA.

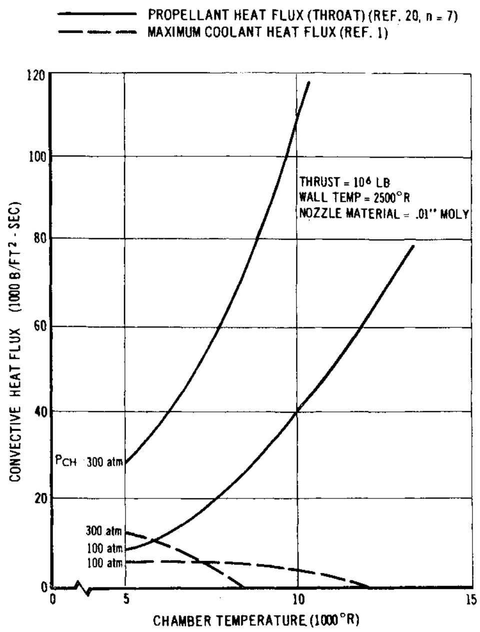

Fig. 1 Comparison of maximum propellant and coolant convective heat fluxes.

nozzle is shown in Fig. 1. A rise of 5000°R in chamber temperature over the solid-core temperature can increase the heat flux by a factor of four. The cooling problem is further aggravated by thermal radiation from the propellant. On the other hand, the cooling capability of convection cooling (dashed lines) decreases rapidly with chamber temperature because of the high temperature drop through the nozzle wall. Hence, regenerative cooling is inadequate at chamber conditions now being considered for the gas-core system.

This paper presents an investigation of mass injection through a porous wall as a possible means of handling these ultrahigh heat loads. The thermal effectiveness of this technique over convective cooling is inherent in two mechanisms: 1) efficient heat transfer from the wall to the infiltrating coolant caused by the intimate fluid-solid contact in a porous medium of high specific surface area, and 2) the local injection of mass into the boundary layer, which tends to decrease the local heat transfer to the wall.

The application of mass injection for cooling rocket engines was recognized as early as 1929 by Oberth. The earliest experiments were conducted by Goddard[4] (1930), Meyer-Hartwig[5] (1940), and Skoglund[6] (1942). Basically, these experiments were conducted to demonstrate feasibility of transpiration cooling.

The analytical investigation of mass-transfer cooling appears to have had its conception around the late 1940's. Probably the most complete analysis of heterogeneous, laminar boundary layers is attributed to Baron,[7] who used a similarity transformation to obtain total differential equations. Other investigators who have approached the problem similarly to Baron are Eckert[8] and Szicklas.[9] Knuth[10] introduces the concept of reference states, thus enabling the use of constant property solutions. Rubesin[11] analyzed mass injection in a turbulent, compressible boundary layer by an integral momentum approach, first for air-to-air and later for the injection of a dissimilar gas. Ness[12] considers the injection of a foreign gas into a compressible, turbulent boundary layer on a flat plate and presents results for the injection of helium into undissociated air. In an attempt to obtain reference state solutions for turbulent flows with mass transfer, Knuth[13] used his reference temperature for laminar flow and a derived Reynolds analogy to correlate existing experimental data, particularly the data of Bartle and Leadon.[14]

No recent analysis of mass-transfer cooling in axisymmetric nozzles appears to have been reported in the open literature. The following analysis considers homogeneous mass injection into a compressible, turbulent boundary layer with an axial pressure gradient. Thermal radiative heat transfer from the freestream is also considered.

Analysis

The mathematical model is characterized in Fig. 2. A homogeneous coolant (i.e., the coolant is chemically identical to the mainstream) is injected through a porous wall normal to the mainstream at a mass velocity G. It is assumed that the nozzle contour, freestream conditions, wall temperature, and initial boundary-layer thickness are specified. Heat is assumed to be transferred to the wall by simultaneous convection and radiation from the propellant.

Neglecting axial conduction in the wall, the enthalpy rise of the coolant must be equal to the heat transfer to the wall. By assuming that the specific heat of the coolant is constant, a heat balance at the gas-wall interface yields the following equation:

$$GC_{p_c}(t_W - t_{ci}) = \dot{q}_C + \dot{q}_R \tag{1}$$

An investigation of Eq. (1) indicates that four parameters must be determined, assuming that the inlet coolant temperature is specified, i.e., G, t_W, $\dot{q}_C$, and $\dot{q}_R$. It is usually convenient to divide the analysis into two phases: 1) the determination of the coolant and wall temperature distribution, and 2) a boundary-layer analysis to determine the heat transfer with mass injection.

Wall and Coolant Temperature Distribution

The temperature distribution of the coolant and the solid material in the porous wall will depend upon the initial thermodynamic state of the injected fluid. If the coolant initially enters the wall as a liquid, and vaporization occurs within the wall or boundary layer, more heat capacity is realized than if the coolant enters in the gaseous phase. However, the application of homogeneous mass injection is concerned primarily with propulsion systems utilizing hydrogen. Chamber pressures usually considered for these systems (~1000 psia) will require coolant inlet pressures of the same order in the throat and convergent regions of the nozzle, which are substantially above the critical pressure of hydrogen (P_{cr} = 188 psia). For this reason, the coolant will be considered to exist in the gaseous phase throughout the analysis.

Various analyses concerning the heat-transfer process in porous walls have been reported in the literature.[15, 16] Bernicker[15] assumes that the random, capillary-like passages in the wall are replaced by small, uniform, cylindrical passageways and that the heat conducted through the coolant is negligible. He also determines an empirical relationship for the internal heat-transfer coefficient. For large values of the internal heat-transfer coefficients, it is found that the coolant and wall temperatures are indistinguishable throughout most of the wall, and that a simplified asymptotic solution describes the coolant and wall temperature distribution.

For the present application, estimated values of the internal heat-transfer coefficient for hydrogen are sufficiently large enough to warrant the use of the asymptotic solution for the temperature distribution. The temperature distribution given in Ref. 15 is

$$\frac{t - t_{ci}}{T_W - t_{ci}} = \frac{\exp(\eta\lambda/\beta) + P/(1 - P)}{\exp(\lambda/\beta) + P/(1 - P)} \tag{2}$$

where

$$\eta = y/a \qquad \lambda/\beta = GC_{p_c}a/K_W(1 - P)$$

Since it is assumed that the wall temperature is specified as a design parameter, Eq. (1) is reduced to three unknowns, since $t_W = T_W$ at the gas-wall interface. The heat fluxes and coolant flow rate are then determined from the boundary-layer analysis. As will be seen later, Eq. (2) will be useful for calculating the pressure drop across the porous wall.

Boundary-Layer Analysis

The classical method for predicting heat transfer in nozzles without mass injection has been that of employing the integral-momentum and energy equations.[17–19] The apparent success obtained in correlating experimental data led to the use of this approach for the present analysis. The integral-momentum approach has been extended to account for mass injection, and the influence of blowing on the transverse velocity profile and skin-friction correlation has been arbitrarily accounted for by relations employing an unknown parameter as suggested by Persh.[20] Reference states are used to account for changes in transport properties across the boundary layer.

The following assumptions are made in the analysis: 1) the coolant and propellant are chemically identical, 2) dissociation in the boundary layer affects only the driving potential relative to the heat flux, 3) the boundary-layer velocity profile is given by $U/U_\infty = (y/\delta)^{1/n}$, 4) the Crocco quadratic form of the temperature profile applies, and 5) a modified form of Reynolds' analogy is valid for the convective heat flux.

The derivation of the integral-momentum equation essentially follows the procedure of Bartz[17] except that the boundary condition $y = 0$, $\rho V = G$ is imposed on the solution. The resulting equation may be expressed as

$$\frac{d\theta}{dx} = \frac{C_f}{2} + F - \theta\left\{\frac{1}{M}\frac{dM}{dx}\frac{[(\delta^*/\theta) + 2 - M^2]}{1 + [(\gamma - 1)/2]M^2} + \frac{1}{D}\frac{dD}{dx}\right\} \tag{3}$$

where the displacement thickness δ^* is given by the relation

$$\frac{\delta^*}{\delta} = \int_0^1 \left(1 - \frac{\rho U}{\rho_\infty U_\infty}\right) d\left(\frac{y}{\delta}\right) \tag{4}$$

and the momentum thickness is defined as

$$\frac{\theta}{\delta} = \int_0^1 \frac{\rho U}{\rho_\infty U_\infty}\left(1 - \frac{U}{U_\infty}\right) d\left(\frac{y}{\delta}\right) \tag{5}$$

The equation for δ^*/δ and θ/δ requires only the knowledge of the temperature and velocity profile in the boundary layer. The necessity to consider a concentration gradient in the boundary layer is eliminated by the third assumption. The velocity profile exponent n is to be determined by experiment.

Under the assumption of the Crocco temperature-profile relationship, the temperature profile in the boundary layer is given in Ref. 17 as

$$T/T_\infty = a(1 + b\eta^{1/n} - c\eta^{2/n}) \tag{6}$$

where

$$a = \frac{T_W}{T_\infty} \qquad b = \frac{T_{CH}}{T_W} - 1$$

$$c = \frac{\gamma - 1}{2}M^2\frac{T_\infty}{T_W} \qquad \eta = \frac{y}{\delta}$$

Assuming the perfect gas relationship for the density, and the pressure across the boundary-layer thickness as being constant, Eqs. (4) and (5) may be written as

$$\frac{\delta^*}{\delta} = \int_0^1 \left[1 - \frac{\eta^{1/n}}{a(1 + b\eta^{1/n} - c\eta^{2/n})}\right] d\eta \tag{7}$$

$$\frac{\theta}{\delta} = \int_0^1 \frac{\eta^{1/n}(1 - \eta^{1/n})}{(1 + b\eta^{1/n} - c\eta^{2/n})} d\eta \tag{8}$$

The expression for skin friction is taken from Ref. 20, but has been modified relative to the evaluation of the properties

$$C_f/2 = (20n)^{(1-n)/(1+n)}(\mu_*/\rho_* U_\infty\delta)^{2/(n+1)} \tag{9}$$

where the viscosity and density are evaluated at the reference temperature of Knuth[13]

$$T_* = 0.5T_W + 0.5T_\infty + 0.17r_0(U_\infty^2/2gC_p) + 0.08Pr(G/\rho_\infty U_\infty)(T_W - T_\infty) \tag{10}$$

The molecular weight used to evaluate the density is based on an arithmetic average of the mole fraction of the propellant at the freestream and the wall

$$m_* = \{[(X_\infty + X_W)/2]_1 m_1\} + [(X_\infty + X_W)/2]_2 m_2 \tag{11}$$

The convective heat flux is obtained from a modified form of Reynolds analogy, which differs from the usual form in two ways: 1) the effect of dissociation in the boundary layer has been accounted for by applying the results of Dorrance,[22] which were determined empirically for heat transfer in compressible, turbulent boundary layers on flat plates, and 2) the density, Prandtl number, and Lewis number are evaluated at the reference temperature given by Eq. (10).

Applying the preceding conditions to the original Reynolds analogy given in Ref. 22, the equation for the convective heat flux is

$$q_c = \frac{\rho_* U_\infty}{Pr_*^{2/3}}(H_{AW} - H_W)\frac{C_f}{2}\left[2\left(\frac{1}{1 + C_\infty}\right)^{1/7} - 1\right] \times \left[1 + (Le_*^{2/3} - 1)\frac{C_\infty D}{(H_{AW} - H_W)}\right] \tag{12}$$

where

$$H_{AW} = H_\infty + r_0\frac{u_\infty^2}{2g} \qquad C_\infty = \frac{(x_\infty)_1 m_1}{[(x_\infty)_1 m_1 + (x_\infty)_2 m_2]}$$

The following assumptions were made for the determination of the radiative heat flux: 1) the gas is a nongrey, isotropic, homogeneous medium; 2) the wall is a diffuse, grey emitter and absorber; 3) the contribution of the radiative flux from adjacent wall segments is small as compared with the flux from the gas; 4) the temperature profile in the gas is unaffected by radiation; and 5) heat transfer is in the radial direction only. Based on the previous assumptions, the expression for the radiative heat flux is[33]

$$q_R = \bar{\alpha}_W \int_0^\infty \int_0^{\tau_D} 2E_{B\omega}(t)\xi_2(t)dtd\omega - \bar{\epsilon}_W\sigma T_W^4 \tag{13}$$

where $E_{B\omega}$ is Planck's function for blackbody radiation of wave number ω and temperature T. According to quantum theory

$$E_{B\omega} = 2\pi hc^2\omega^3/[\exp(hc\omega/KT) - 1] \tag{14}$$

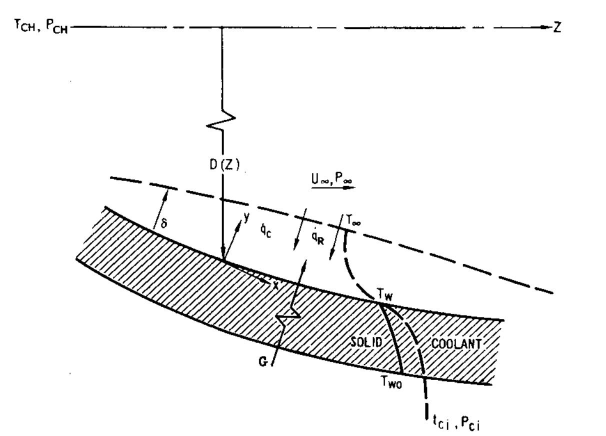

Fig. 2 Analytical model for transpiration-cooled nozzle.

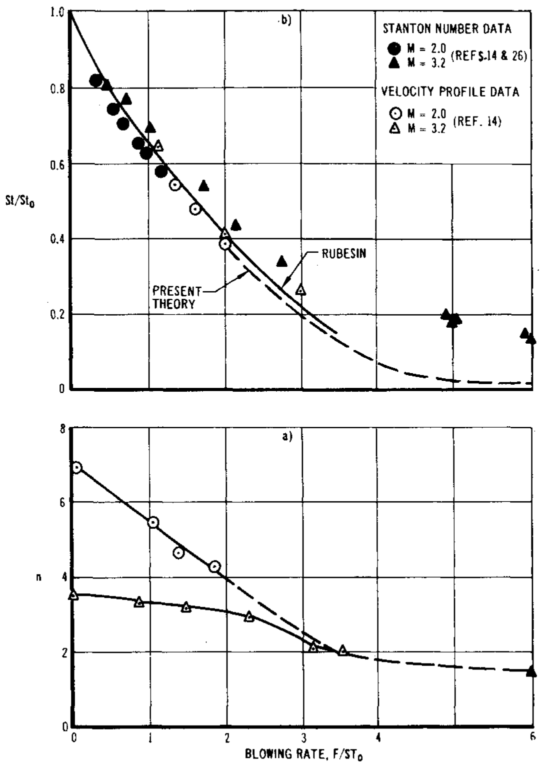

Fig. 3 Velocity profile exponent and Stanton number reduction.

$\xi_2(t)$ is the second integroexponential function where

$$\xi_2(t) = \int_1^\infty \frac{e^{-t\mu}}{\mu^2}\, d\mu \tag{15}$$

and t is the optical thickness

$$t = \int_0^y \kappa_\omega[T(y)]dy \tag{16}$$

$$\tau_D = \int_0^D \kappa_\omega[T(y)]dy \tag{17}$$

Values of the absorption coefficient of hydrogen (as a function of temperature, pressure, and wavelength) were taken from Ref. 21. Equations (13–17) were evaluated by numerical integration techniques. The temperature profile in the boundary layer was determined by Eq. (6) in every case except for that of 20,000°R. At 15,000°R and below, at least 90% of the radiant energy that reaches the wall is from the freestream, and thus there is a negligible effect of radiation on the

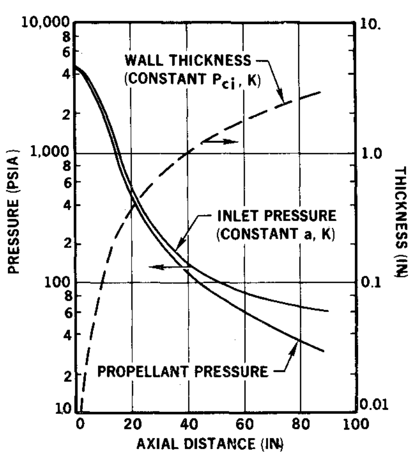

Fig. 4 Coolant metering techniques.

temperature profile in the boundary layer. At 20,000° R the absorption coefficient of hydrogen is such that most of the energy is emitted from within the boundary layer. It was felt beyond the scope of the current study to investigate the effect of radiation in the boundary layer. It was assumed for the 20,000°R case that the gas radiates as a blackbody at the freestream temperature, which is a conservative estimate of the radiative heat load to the wall. The effect of radiation on the velocity profile was not considered, thereby representing an optimistic estimate of the convective heating. However, the effectiveness of transpiration cooling in reducing the convection will minimize this effect.

The preceding equations were programed on the IBM 7090 computer, using the formula translation (FORTRAN II) system. Essentially, the program treats the nozzle as a series of parabolic segments, and determines the boundary-layer parameters, heat transfer, coolant mass velocity, etc., at each segment. The integral-momentum equation is solved by a finite-difference technique.

Comparison of Results

As with any theory, the proof of validity rests on comparison with experimental results as well as with its internal consistency. In this analysis, as with the case of most analyses dealing with heat transfer in turbulent flows, there arose the necessity to include certain parameters that must be determined by experiment, in this case, the parameter n. In essence, Rubesin[11] encountered similar difficulty in his analysis. Within the framework of his assumptions, Rubesin had to assume values of the mixing length parameter and velocity at the laminar-turbulent interface. Therefore, the following discussion is confined to the determination of suitable values of n (assuming such values exist) from existing experimental data.

The effects of mass injection on the heat transfer is usually shown in terms of two parameters: 1) the Stanton number reduction St/St_0, which is the ratio of Stanton number with mass injection to that without injection, and 2) the recovery temperature. When the former is plotted as a function of a blowing parameter defined as $(G/\rho_\infty U_\infty)/St_0$, the effects of Mach number and Reynolds number are minimized.[14]

The paucity of heat-transfer data in transpiration-cooled nozzles made it necessary to rely heavily on flat plate data. The data of Bartle and Leadon[14, 26] appear to be the most reliable to date for nitrogen injections into air with freestream Mach numbers of 2.0 and 3.2. (Other experimental investigations include those of Leadon and Scott[23] and Rubesin.[24])

From the velocity profile data of Ref. 14, the authors determined the effect of blowing on the velocity exponent (Fig. 3a). Data were given up to $F/St_0 = 1.96$ for Mach 2 and $F/St_0 = 3.53$ for Mach 3.2. The curve for Mach 2 was extrapolated until it intersected the Mach 3.2 curve. These data were then used in conjunction with the present theory to generate Stanton number reduction data, the results of which are shown in Fig. 3b. The comparison between the experimental and calculational results is extremely good, thus substantiating the theory. In order to obtain data for n at blowing rates greater than 3.5, the authors used the St/St_0 (Ref. 26) data at $F/St_0 = 6$ and worked backwards. A straight line variation of n from an F/St_0 of 3.5 to 6.0 was assumed. The curve was extrapolated to obtain n for F/St_0's greater than 6; however, a minimum value of $n = 1$ was used for calculations. This method appears to be an extremely useful tool, especially if more data on n (or velocity profile) as a function of Mach number and Reynolds number were available.

In regarding the calculations for the parametric study, Stanton numbers for the no-blowing case were based on $n = 7$ for two reasons: 1) it should represent a relatively conservative estimate of the heating rate, and 2) the initial boundary-layer velocity profile for the Mach 2 case[14] follows $n = 7$.

Also the curve of n vs F/St_0 for Mach 2 was used since Mach 2 represents an average Mach number for the parametric study.

Coolant Metering Considerations

Once the axial coolant flow distribution has been determined from heat-transfer considerations, the pressure-flow relationship can be obtained from the Green[25] equation

$$-\rho dP/dy = \alpha\mu G + \beta G^2 \tag{18}$$

where α and β are the viscous and inertia resistances of the porous wall. By assuming the ideal gas law, Eq. (18) can be expressed as

$$-PdP = Rt(y)[\alpha\mu G + \beta G^2]dy \tag{19}$$

Upon inserting the expression for the coolant temperature distribution, integrating between $y = 0$ and $y = a$, and applying the boundary conditions

$$\begin{gathered} y = 0 \qquad P = P_\infty \qquad y = a \qquad P = P_{ci} \\ P_{ci}^2 - P_\infty^2 = 2Ra\mu G\bar{t}(\alpha + \beta G) \end{gathered} \tag{20}$$

where

$$\bar{t} = \frac{(T_W - t_{ci})}{e^{\lambda/\beta} + \bar{P}}\left[\frac{e^{\lambda/\beta} - 1}{\lambda/\beta} + \bar{P} + \frac{t_{ci}}{T_W - t_{ci}}(e^{\lambda/\beta} + \bar{P})\right]$$

Generally the resistance coefficients can be combined in the form of one constant, namely, the permeability coefficient, whereby G must be raised to some power between 1 and 2. Thus

$$P_{ci}^2 - P_\infty^2 = (2Ra\mu\bar{t})G^{n'}/k \tag{21}$$

where n' is an empirically determined exponent.

An investigation of Eq. (21) indicates that there are various possibilities of obtaining the required flow distribution. Since the axial back pressure distribution (P_∞) is fixed by the propellant, either the inlet pressure (P_{ci}), wall thickness (a), or permeability coefficient (k) must be varied axially.

If the physical properties of the porous wall are fixed, a typical axial coolant-inlet pressure distribution that results is shown in Fig. 4. In order to achieve such an axial pressure distribution, it would become necessary to compartment the coolant channels along the length of the nozzle and regulate the pressure in each compartment. The disadvantage of such a technique is the added complexity and weight as compared with other techniques. Figure 4 also shows a typical distribution for a case in which wall thickness is varied. As noted, the wall thickness may increase by several orders of magnitude at the divergent end of the nozzle because of the low flow rate and low back pressure conditions. Because of the large variation in wall thickness, this technique becomes impractical.

A third alternative is to vary the permeability coefficient of the porous material in the axial direction. This technique is most conducive to porous components produced from metallic wire cloth. The variable permeability is obtained by cold-rolling the wire-woven component at different rolling pressures along the length. In an attempt to determine the feasibility of this concept, the Douglas Company contracted Bendix Filter Division to manufacture Poroloy cylinders with a variable permeability in the axial direction. Poroloy is the trade name associated with a high-quality porous metal made by winding fine, flattened wire into tubular shapes, which is then sintered to produce bonding of the fibers. Bendix successfully produced variable permeability Poroloy tubes by using an air-bearing supported ball roller actuated by a template-controlled air source. The actual air-flow distribution is shown along with the theoretical results in Fig. 5 and is seen to agree fairly well. This technique definitely shows promise in yielding a lightweight, simple metering system for transpiration-cooled nozzles.

Fig. 5 Flow distribution in Poroloy tube (sample no. B-1).

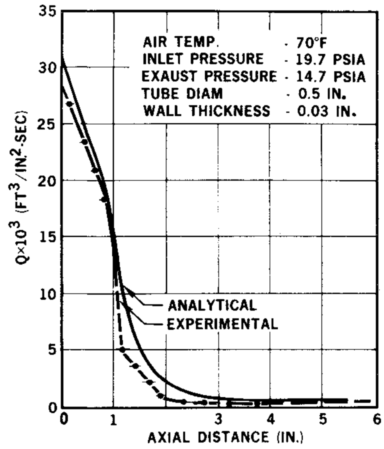

Gas-Core Parameter Study

The feasibility of the gas-core reactor concept will be dependent upon the solution of various technological problems. The major effort at present is being directed toward two basic problems: 1) efficient separation of the fuel and propellant and 2) the attainment of efficient thermal energy exchange between the gaseous fuel and hydrogen. The resolution of these problems will definitely influence the selection of the optimum operating conditions. However, the degradation in total system performance caused by maintaining the nozzle wall at a safe structural temperature does not appear to have received sufficient attention. The extent to which I_{sp} is reduced would appear to be a major factor in determining optimum operating conditions.

To this end, a parametric study was conducted over a range of chamber and wall temperatures for a typical gas-core system utilizing a transpiration-cooled conical nozzle. Chamber pressure was fixed at 300 atm. (Pressure exerts a secondary effect on total coolant flow rate because coolant flow rate is proportional to the product of heat flux $\dot{q}\alpha\ P_{CH}{}^{.8}$ and nozzle surface area $A_s\alpha P_{CH}{}^{-1}$.) Thrust was fixed at 10^6 lb. The assumed nozzle comprises a 45° convergent cone and a 15° divergent cone joined together by a smooth curve (Fig. 6). A cylinder was assumed to precede the convergent nozzle so as to allow sufficient development of the boundary layer prior to the entrance of the nozzle, but the cylinder was not included in the calculations of total coolant flow rate. The throat radius of 6.18 in. was calculated on the basis of a thrust coefficient of 1.89. This value corresponds to an exit area ratio of 50, assuming equilibrium expansion. Additional assumptions that are expanded upon in later sections are:

1) The propellant undergoes equilibrium, isentropic, one-dimensional expansion.

2) The nozzle is composed of a series of longitudinal porous tubes made from 0.02-in. molybdenum alloy. The thickness was determined on the basis of maximum hoop stress in the tube.

3) Transpiration-cooling is utilized over the surface area of the nozzle which cannot be regeneratively cooled. The minimum regeneratively cooled area ratio ϵ_{RC} is a function of chamber temperature, and is determined in a later section.

4) The average I_{sp} is determined on the basis of the coolant entering with a total temperature equal to that of the wall and completely mixing with hot central gas.

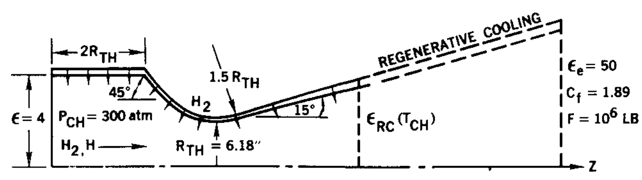

Fig. 6 Nozzle contour for parameter study.

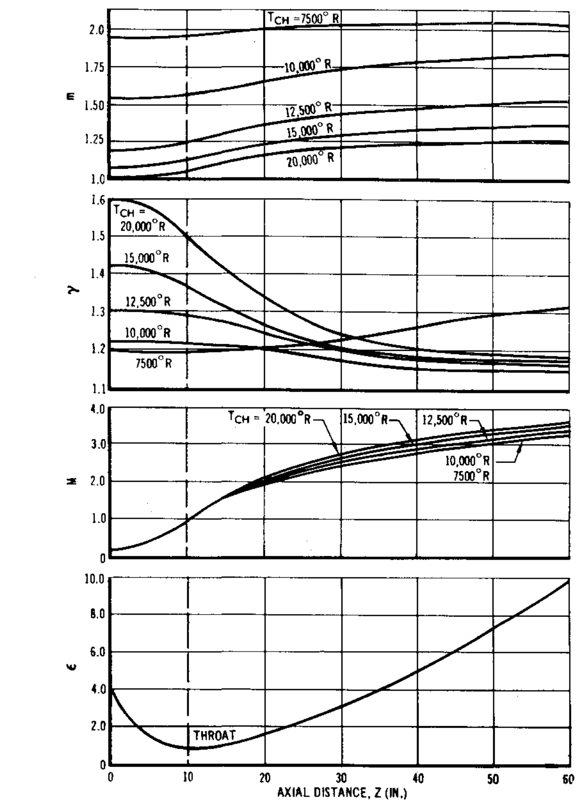

Fig. 7 Thermodynamic freestream properties in nozzle (equilibrium flow).

Determination of Freestream Properties

Bray[27] has shown that flow passes from a near-equilibrium to a near-frozen state in a relatively short section of the nozzle, so that a reasonably accurate solution may be obtained by assuming equilibrium flow up to the "freezing" area ratio and frozen flow for the remainder. Typical values[28] for hydrogen over a limited range of temperature and pressure are shown in Table 1. It is not possible to extrapolate the preceding data to the conditions being considered for the parametric study, but it is noteworthy that ϵ_f increases with pressure because of a decrease in the recombination rate constant. Since the chamber pressure being considered is several orders of magnitude higher than the values shown previously, it is suspected that the assumption of equilibrium flow is valid over the range of ϵ_{RC}. Therefore, freestream properties were determined by a Douglas computer program that computes the composition and thermodynamic properties of gases undergoing equilibrium, isentropic expansion using the method of solution described in a NACA report.[30] Thermodynamic properties are obtained from Joint Army-Navy-Air Force (JANAF) thermochemical tables[31] (<10,800°R) and the auxiliary Douglas program using statistical mechanics (10,800°–45,000°R).

Table 1

T_{CH}, °R	P_{CH}, atm	ϵ_f
6360	0.85	1.3
6210	0.81	1.5
7770	2.45	2.4

The results of the computer runs are shown as a function of axial distance in Fig. 7. As noted, chamber temperature exerts little effect on the Mach number distribution, but does effect the specific heat ratio. An average specific heat ratio was used in the computer program. Transport properties of H_2 were obtained from Ref. 29.

Determination of ϵ_{RC}

The heat-removal capability of regenerative cooling is limited by the thermodynamic consideration that the coolant must always be subsonic. Kramer and Sanders[1] have shown that there is an optimum set of coolant conditions which maximizes the amount of heat removal and minimizes the coolant pressure drop. These conditions were found to be: 1) coolant Mach number = 0.55 and 2) coolant bulk temperature to wall temperature ratio = 0.25.

Using the preceding set of conditions, the limiting area ratio to which the nozzle can be cooled by convection was found as a function of chamber temperature. Gas-side wall temperature was fixed at 2500°R.

The three equations used in the analysis were: 1) heat flux to the wall

$$\dot{q}_G = h_G(H_{AW} - H_W)$$

where

$$h_G = 0.026 Pr_*^{-2/3}[\dot{w}_0/(A_{th}\epsilon)]^{0.8}[\mu_*/(D_{th}\epsilon^{1/2})]^{0.2} \times [(T_\infty m_*)/(T_* m_\infty)]^{0.8}$$

2) temperature drop through the wall

$$T_{W0} = T_W - \dot{q}_G(t_W/K_W)$$

and 3) heat flux to the coolant

$$\dot{q}_c = h_c(T_{W0} - t_c)$$

where

$$T_* = 0.5\,(T_{W0} + t_c)$$

$$h_c = 0.023 C_{p*} Pr_*^{-2/3}(\rho_* V_c)^{0.8}(\mu_*/d_{th}\epsilon^{1/2})^{0.2}$$

These three equations were solved simultaneously for the area

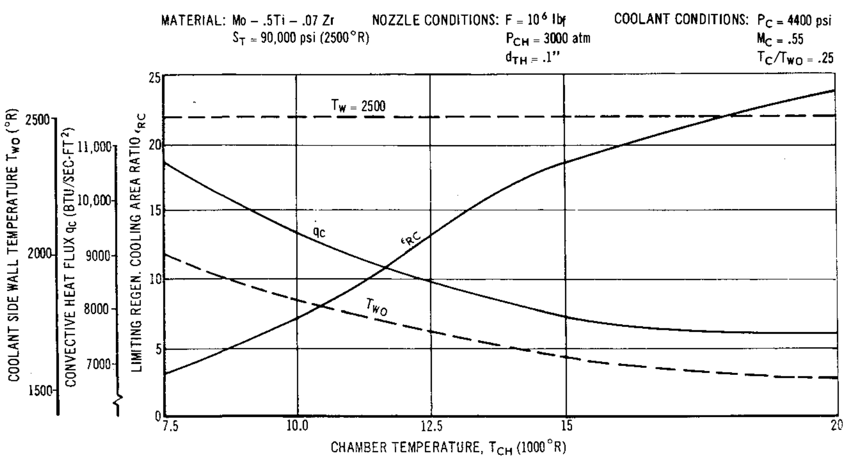

Fig. 8 Limiting parameters of regenerative cooling.

ratio for the condition that the gas-side heat flux is exactly equal to the coolant-side heat flux. The results of the computations are shown in Fig. 8. It should be noted that radiative heat flux from the propellant was assumed to be negligible.

Results of Transpiration-Cooling Analysis

The computer program considers the nozzle as a series of parabolic segments and computes the boundary-layer thickness, heat fluxes, coolant mass velocity, velocity exponent, and other heat-transfer parameters at the end of each segment. The radiative heat flux is calculated by the methods described previously. Typical values for the porous-wall solar absorptivity and emissivity of 0.6 and 0.2, respectively, were assumed.[32]

The variations in the heat flux with and without blowing are shown in Fig. 9 for a wall temperature of 2500°R. The main figure shows the total heat flux (convective plus radiative) for three chamber temperatures. Blowing is seen to reduce the convective heat load substantially. For instance, the convective heat flux with blowing is 16,000 B/sec-ft^2 at the throat (T_{CH} = 15,000°R), whereas it is 205,000 B/sec-ft^2 without blowing, thus representing a decrease by an order of magnitude.

The variation of the blowing parameter with axial distance is shown in Fig. 10. Higher blowing rates are required at 15,000° and 20,000°R in the region of high radiative heat loads. The blowing rate at the entrance to the nozzle for 20,000°R is about 37. As radiation becomes less important in the divergent nozzle, the blowing rate approaches a constant value. This result would be expected for a flat plate and indicates the small effect of a pressure gradient on the Stanton number reduction.

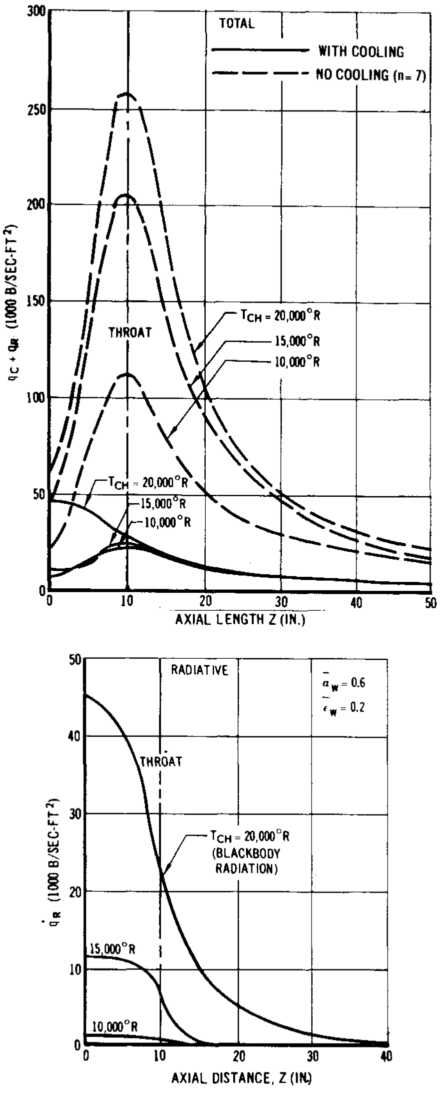

Fig. 9 Total and radiative heat flux distribution in nozzle, T_W = 2500°R.

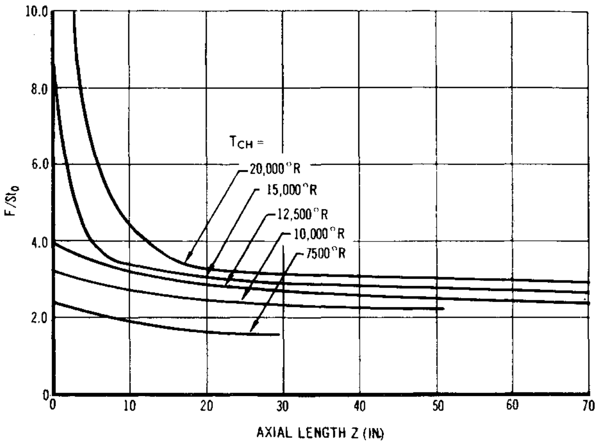

Fig. 10 Variation of blowing parameter in the nozzle, T_W = 2500° R.

Another important parameter of interest is the backwall temperature in the coolant tube since thermal stress will be directly proportional to the temperature drop. The backwall temperature as a function of axial length is shown in Fig. 11 for a typical chamber temperature of 15,000°R (chamber temperature has a small effect on T_{W0} since the heat fluxes are nearly the same for all values of T_{CH}). The maximum thermal stress exists at the throat and increases with increasing wall temperature. For T_W = 2000°R, the maximum thermal stress is about equal to the tensile strength of molybdenum at 2000°R. However, at the higher wall temperature, thermal stress far exceeds the tensile strength. Thus it appears that thermal stress is a definite limitation considering the design wall temperature (2000°R being the upper limit for this study).

The variation of coolant mass velocity G with axial distance is similar in shape to that of the heat flux, as would be expected for a constant wall temperature. Of major interest is the total coolant flow rate, obtained by numerically integrating the individual mass velocities over the area. The total coolant flow rate is

$$\dot{w}_c = N_t \sum_{i=1}^{N} \frac{(G_i + G_{i+1})}{2} \frac{A_t}{2} \tag{22}$$

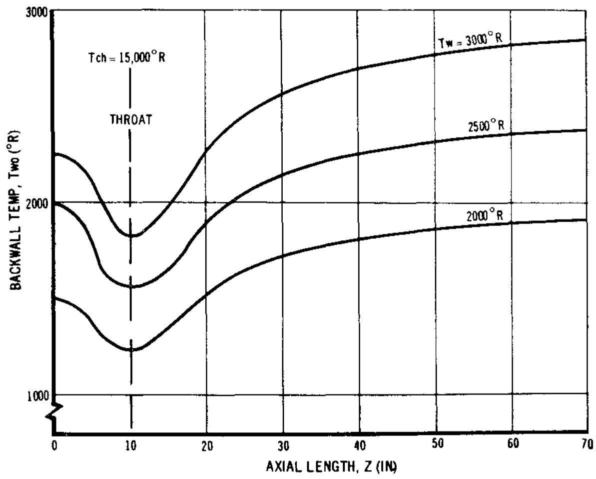

Fig. 11 Variation of backwall temperature in porous tube.

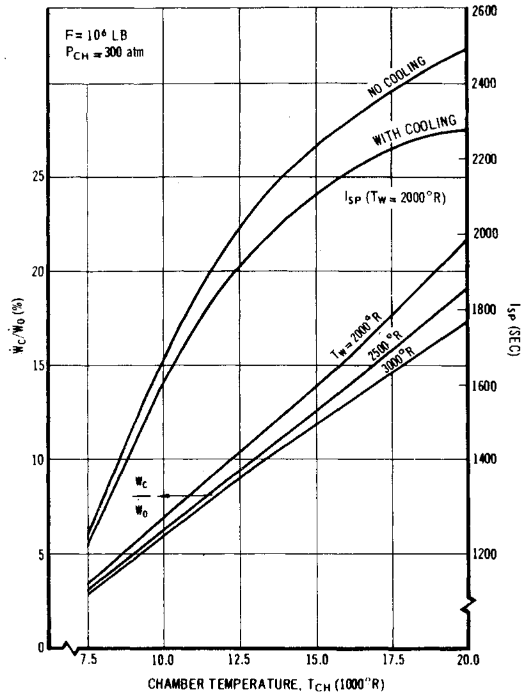

Fig. 12 Total coolant flow and specific impulse of a transpiration-cooled nozzle system.

where

$$A = \pi(\bar{d}_i + \bar{d}_{i+1})(\Delta S/2) \tag{22a}$$

$$\bar{d}_i = \frac{\pi D_i}{(N_t - \pi/2)}\left(\frac{dx}{dz}\right)_i - t_W \tag{22b}$$

$$\Delta S = [\tfrac{1}{4}(D_{i+1} - D_i)^2 + (Z_{i+1} - Z_i)^2]^{1/2} \tag{22c}$$

The results of the calculation are shown in Fig. 12 (nozzle only; the upstream cylindrical portion was not considered). The coolant flow rate is shown as a ratio of coolant flow to the total propellant flow rate

$$\dot{w}_0 = F/I_{sp}(T_{CH}) \tag{23}$$

Coolant flow rates of the order of 20% of the total propellant flow are required at the chamber temperatures being considered at present for the gas-core system (about 20,000°R).

A parameter of paramount importance is the average I_{sp} of the system. Specific impulse was calculated on the basis of complete mixing of the coolant entering at the wall temperature. This method yields an upper limit on I_{sp}. The equation for determining the average specific impulse is

$$I_{sp}^{tc} = \left[\left(1 - \frac{\dot{w}_c}{\dot{w}_T}\right) I_{sp}{}^2(T_{CH}) + \left(\frac{\dot{w}_c}{\dot{w}_T}\right) I_{sp}{}^2(T_W)\right]^{1/2} \tag{24}$$

The specific impulse is shown in Fig. 12 for a wall temperature of 2000°R. It can be seen that consideration of the nozzle cooling problem has an effect on the system performance. For a chamber temperature of a typical gas-core system, a reduction of 222 sec can be expected, representing a 9% loss in performance.

Two major tasks must be accomplished before anything more significant can be stated: 1) obtain data over a broad range of blowing rates, Mach numbers, and Reynolds numbers in nozzles, and evaluate this data in terms of n; and 2) evaluate the specific effect of gas injection on over-all radiative heating rate to the wall.

Concluding Remarks

The effect of homogeneous mass injection on heat transfer in an axisymmetric nozzle was analyzed and the results were used to conduct a parameter study for a typical conical nozzle associated with a gas-core nuclear system. At chamber temperatures now being considered for gas-core applications (up to 20,000°R), the specific impulse was predicted to be degraded by about 9% because of nozzle cooling requirements.

References

[1] Kramer, E. L. and Sanders, A., "Nozzle design analysis for nuclear rocket applications," IAS Paper 62-59 (1962).

[2] Benser, W. A. and Graham, R. W., "Hydrogen convective cooling of rocket nozzles," American Society of Mechanical Engineers Paper 62-AV-22 (1962).

[3] Plunkett, T. F. and Holl, R. J., "Nuclear analysis of gaseous core reactors," Douglas Aircraft Co. Rept SM-44041 (1963).

[4] Goddard, R. H., *Rocket Development* (Prentice-Hall, Inc., New York, 1948), p. 13.

[5] Meyer-Hartwig, F., "The cooling of highly loaded surfaces by a coolant forced through the pores of the material," FB 1470, Volkenrode Transl. L.F 3 (December 1940).

[6] Skoglund, V. G., U. S. Patent 2,354,151 (1942).

[7] Baron, J. R., "The hetrogeneous laminar boundary layer," Rand Mass Transfer Symposium, Santa Monica, Calif. (June 1957).

[8] Eckert, E. R. G., Schneider, P. J., Hayday, A. A., and Larson, R. M., "Mass transfer cooling of a laminar boundary layer by injection of a light-weight foreign gas," Jet Propulsion **28**, 34–39 (1958).

[9] Szicklas, E. A. and Banas, C. A., "Mass transfer cooling in compressible laminar flow," Rand Mass Transfer Symposium, Santa Monica, Calif. (June 1957).

[10] Knuth, E. L., "Use of reference states and constant-property solutions in predicting mass-, momentum-, and energy-transfer rates in high-speed laminar flows," Intern. J. Heat Mass Transfer **6**, 1–22 (1963).

[11] Rubesin, M. W., "An analytical estimation of the effects of transpiration-cooling on the heat transfer and skin friction characteristics of a compressible, turbulent boundary layer," NACA TN 3341 (1954).

[12] Ness, N., "Foreign gas injection into a compressible, turbulent boundary layer on a flat plate," J. Aerospace Sci. **27**, 321–333 (1960).

[13] Knuth, E. L., "Recent studies on the use of reference states in predicting transport rates for high-speed flows with mass transfer," *Proceedings of the 1963 Heat Transfer and Fluid Mechanics Institute* (Stanford University Press, Stanford, Calif., June 1963), pp. 27–43.

[14] Bartle, E. R. and Leadon, B. M., "The compressible turbulent boundary layer on a flat plate with transpiration cooling," Convair Scientific Research Labs. Rept. 11 (1961).

[15] Bernicker, R. P., "An investigation of porous wall cooling," American Society of Mechanical Engineers Paper 60-WA-233 (1960).

[16] Hawkins, T. D., "Transpiration and film cooling for solid propellant rocket nozzles," United Nuclear Corp. Rept. NDA 2150-1 (1961).

[17] Bartz, D. R., "An approximate solution of compressible, turbulent boundary layer development and convective heat transfer in convergent-divergent nozzles," American Society of Mechanical Engineers Paper 54A153 (1954).

[18] Elliot, D. G., Bartz, D. R., and Silver, S., "Calculation of turbulent boundary-layer growth and heat transfer in axi-symmetric nozzles," Jet Propulsion Lab. TR 32-387 (1963).

[19] Neuman, H. and Bettinger, P., "A comparative analysis of convective heat transfer in a nuclear rocket nozzle," NASA TND-1742 (1963).

[20] Persh, J. and Lee, R., "A method for calculating turbulent boundary layer development in supersonic and hypersonic nozzles including the effects of heat transfer," U. S. Naval Ordnance Lab. Rept. 4200 (1956).

[21] Krascella, N. L., "Tables of the composition, opacity, and thermodynamic properties of hydrogen at high temperatures," NASA SP-3005 (1963).

[22] Dorrance, W. H., "Dissociation effects upon compressible turbulent boundary layer at $M = 3$," ARS J. **31**, 61–70 (1961).

[23] Leadon, B. M. and Scott, C. J., "Transpiration-cooling experiments in a turbulent boundary layer at $M = 3$," J. Aeronaut. Sci. **23**, 798–799 (1956).

[24] Rubesin, M. W., Pappas, C. C., and Okuno, A. F., "The effect of fluid injection on the compressible turbulent boundary layer—preliminary tests on transpiration cooling of a flat plate at $M = 2.7$ with air as the injected gas," NACA A55119 (1955).

[25] Green, L., Jr. and Duwez, P., "Fluid flow through porous metals," J. Appl. Mech. **18**, 39–45 (1951).

[26] Bartle, E. R. and Leadon, B. M., "Experimental evaluation of heat transfer with transpiration cooling in a turbulent boundary layer at $M = 3.2$," J. Aerospace Sci. **27**, 78–80 (1960).

[27] Bray, K. N. C., "Atomic recombination in a hypersonic wind-tunnel nozzle," J. Fluid Mech. **6**, 1–32 (1959).

[28] Widawsky, A., Oswalt, L. R., and Harp, J. L., "Experimental determination of the hydrogen recombination constant," ARS J. **32**, 1927–1929 (1962).

[29] Vanderslice, J. T., Weisman, S., Mason, E. A., and Fallon, R. J., "High-temperature transport properties of dissociating hydrogen," Phys. Fluids **5**, 155–164 (1962).

[30] Hoff, V. N., Gordon, S., and Morrell, V. E., "General method and thermodynamic tables for computation of equilibrium composition and temperature of chemical reactions," NACA 1037 (1951).

[31] "JANAF thermochemical data," Joint Army-Navy-Air Force Thermochemical Panel, Dow Chemical Co., Vol. 1 (1960)

[32] Irvine, T. F., Jr., Hartnett, J. P., and Eckert, E. R. G., "Solar collector surfaces with wavelength selective radiation characteristics," Solar Energy **2**, 12 (1958).

[33] Goulard, R. and Goulard, M., "One-dimensional energy transfer in radiant media," Intern. J. Heat Mass Transfer **1**, 81–91 (1960).

MAY-JUNE 1965 J. SPACECRAFT VOL. 2, NO. 3

A Radiation-Cooled Nuclear Rocket Nozzle for Long Firing Durations

SIDNEY ELKIND*
Arde-Portland, Inc., Paramus, N. J.

A thermal analysis was made of an uncooled nozzle for a 20-min firing. A 15,000-Mw reactor using 1000 psia hydrogen at 4500°R was considered. The analysis consisted of the determination of the transient temperature distribution within the proposed nozzle walls. Modes of heat transfer considered were gas convection, internal heat generation caused by gamma attenuation, conduction, and radiation to space. Design requirements were met by a shielded composite wall of tungsten, graphite, pyrolytic graphite, and René 41.

Nomenclature

c = specific heat
k = thermal conductivity
$\dot{q}$ = rate of volumetric heat generation within wall, Btu/hr-ft^3, at a point whose coordinate is x, at time θ
T = temperature
x = space coordinate, ft
α = thermal diffusivity
δ = wall thickness, ft
ϵ = wall emissivity
θ = time, hr
ρ = density
σ = 0.171×10^{-8} Btu/hr-ft^2-°R^4

Introduction

NUCLEAR rocket systems are currently being considered for many future space missions. In general, the missions are of long duration, requiring high-propulsion power levels. Reliability of all of the components is of paramount importance.

The nozzle not only must withstand the propellant-gas temperature and pressure, but it also must tolerate gamma heating during both operating periods and shutdown. A radiation-cooled nozzle is ideally suited for a nuclear rocket. Besides being inherently reliable, it also has the potential of simplifying the reactor-nozzle interface and making the nozzle independent of the balance of the system. The thermal analysis of a radiation-cooled nuclear nozzle presented in this paper is part of a feasibility study.[1] The specified design conditions include the following: power rating of 15,000 Mw, flow rate (H_2) of 800 lb/sec, inlet diameter of 6 ft, chamber pressure of 1000 psia, chamber temperature of 4500°R, exit-area ratio of 40:1, and "one firing."

The study is divided into two parts: 1) the determination of gamma heating within the wall and 2) the computation of the transient temperature distributions. Both the rate of gamma heating and the wall temperature distribution are functions of the wall configuration. An initial wall configuration was chosen, and transient temperature distributions were computed to determine its capability. The thermal design of the wall was changed, based on the results of this analysis, and the process was repeated until the design objective was achieved.

Heat Transfer

Material Considerations

The choice of materials for the component parts requires the matching of the respective properties and characteristics of proposed materials and the requirements of the parts. A basic consideration was that the materials selected and the design adopted could be fabricated, either at present or in the near future.

The requirements for an uncooled nuclear nozzle are similar to those for uncooled chemical rocket nozzles with the exception of the effects of gamma heating. Solid-propellant

Presented as Preprint 64-389 at the 1st AIAA Annual Meeting, Washington, D. C., June 29–July 2, 1964; revision received November 12, 1964. This paper presents one phase of a study carried out by Arde-Portland, Inc., for NASA Lewis Research Center under Contract No. NAS 3-3670. The author would like to express his appreciation to the Los Alamos Scientific Laboratory for making their QAD IV computer program available for the computation of gamma heating. Thanks are due to both NASA and Arde-Portland, Inc., for permission to publish this paper.

* Senior Heat-Transfer Engineer; now Engineering Specialist, Reaction Motors Division, Thiokol Chemical Corporation. Member AIAA.